Coulomb excitation of ^{29,30}Na: Mapping the borders of the island of inversion

M. Seidlitz,[1] P. Reiter,[1] R. Altenkirch,[1] B. Bastin,[2] C. Bauer,[3] A. Blazhev,[1] N. Bree,[2] B. Bruyneel,[1] P. A. Butler,[4] J. Cederkäll,[5] T. Davinson,[6] H. De Witte,[2] D. D. DiJulio,[7] J. Diriken,[2] L. P. Gaffney,[4] K. Geibel,[1] G. Georgiev,[8] R. Gernhäuser,[9] M. Huyse,[2] N. Kesteloot,[2] T. Kröll,[3,9] R. Krücken,[9,10] R. Lutter,[11] J. Pakarinen,[12] F. Radeck,[1] M. Scheck,[13,14] D. Schneiders,[1] B. Siebeck,[1] C. Sotty,[15] T. Steinbach,[1] J. Taprogge,[1,16] P. Van Duppen,[2] J. Van de Walle,[15,17] D. Voulot,[15] N. Warr,[1] F. Wenander,[15] K. Wimmer,[9,18] P. J. Woods,[6] and K. Wrzosek-Lipska[2,19]

[1]*Institut für Kernphysik, Universität zu Köln, 50937 Köln, Germany*
[2]*Instituut for Kern- en Strahlingsfysica, K.U. Leuven, 3001 Leuven, Belgium*
[3]*Institut für Kernphysik, Technische Universität Darmstadt, 64289 Darmstadt, Germany*
[4]*Oliver Lodge Laboratory, University of Liverpool, Liverpool L69 7ZE, United Kingdom*
[5]*Department of Nuclear Physics, Lund University, SE-221 00 Lund, Sweden*
[6]*School of Physics and Astronomy, University of Edinburgh, Edinburgh EH9 3JZ, United Kingdom*
[7]*European Spallation Source AB, SE-221 00 Lund, Sweden*
[8]*Centre de Spectrométrie Nucléaire et de Spectrométrie de Masse, 91405 Orsay, France*
[9]*Physik Department E12, Technische Universität München, 85748 Garching, Germany*
[10]*Science Division, TRIUMF, Vancouver, British Columbia, V6T 2A3 Canada*
[11]*Department of Physics, Ludwig Maximilian Universität München, 85748 Garching, Germany*
[12]*Department of Physics, University of Jyväskylä, FI-40014 Jyväskylä, Finland*
[13]*School of Engineering, University of the West of Scotland, Paisley PA1 2BE, United Kingdom*
[14]*Scottish Universities Physics Alliance, Glasgow G12 8QQ, United Kingdom*
[15]*Physics Department, ISOLDE, CERN, 1211 Geneva 23, Switzerland*
[16]*Instituto de Estructura de la Materia, CSIC, E-28006 Madrid, Spain*
[17]*Kernfysisch Versneller Instituut, Rijksuniversiteit Groningen, 9747 AA Groningen, Netherlands*
[18]*Department of Physics, Central Michigan University, Mount Pleasant, Michigan 48859, USA*
[19]*Heavy Ion Laboratory, Warsaw University, 02-093 Warsaw, Poland*

(Received 8 October 2013; published 19 February 2014)

Nuclear shell evolution in neutron-rich Na nuclei around $N = 20$ was studied by determining reduced transition probabilities, i.e., $B(E2)$ and $B(M1)$ values, in order to map the border of the island of inversion. To this end Coulomb-excitation experiments, employing radioactive ^{29,30}Na beams with a final beam energy of 2.85 MeV/nucleon, were performed at REX-ISOLDE, CERN. De-excitation γ rays were detected by the MINIBALL γ-ray spectrometer in coincidence with scattered particles in a segmented Si detector. Transition probabilities to excited states were deduced. The measured $B(E2)$ values agree well with shell-model predictions, supporting the idea that in the Na isotopic chain the ground-state wave function contains significant intruder admixture already at $N = 18$, with $N = 19$ having an almost pure two-particle–two-hole deformed ground-state configuration.

DOI: 10.1103/PhysRevC.89.024309 PACS number(s): 21.60.Cs, 23.20.Js, 25.70.De, 29.38.Gj

I. INTRODUCTION

Shell structure is one of the most important frameworks in nuclear physics for describing properties of many atomic nuclei. The key feature of the nuclear shell model is the presence of magic numbers, indicating shell closures. However, recent experimental and theoretical findings indicate that magic numbers are subject to the proton-to-neutron ratio. Thus, well-known shell closures vanish and new magic numbers are revealed when going to more exotic nuclei far from the valley of stability. A first indication for such a vanishing of a shell closure was found in early mass measurements for ^{31,32}Na [1]. Campi *et al*. suggested a deformed ground state for these nuclei [2]. Later shell-model calculations by Warburton *et al*. proposed an anomalous inverted level structure, which is based on two-particle–two-hole (2p2h) neutron cross shell configurations in the ground state [3]. Recent shell-model calculations trace this phenomenon back to the residual nucleon-nucleon interaction [4–8]. The monopole term of the proton-neutron tensor interaction is strongly attractive for the spin-flip proton-neutron partner ($j_>$ and $j_<$) and repulsive for the isospin partner in the same j orbital [8]. It has been shown that the monopole interaction $V^{T=0}_{d_{5/2}d_{3/2}}$ is the most attractive in the *sd* shell [4]. Around ^{30}Si, protons in the $\pi d_{5/2}$ orbital strongly interact with neutrons in the $\nu d_{3/2}$ orbital. The $\nu d_{3/2}$ orbital becomes lower in energy with respect to the $\nu f_{7/2}$ orbital, resulting in the classical magic number $N = 20$ [4]. By removing protons from the $\pi d_{5/2}$ orbital the $V^{T=0}_{d_{5/2}d_{3/2}}$ residual interaction decreases due to the missing $S = 0$ partner protons and the $\nu d_{3/2}$ orbital is shifted to higher energies. The energy gap to the pf shell becomes smaller, causing a new (sub-)shell closure at $N = 16$.

The neutron-rich isotopes of Ne, Na, and Mg are located in the transition region between the shell closures at $N = 20$ and $N = 16$. Compared to ^{34}Si, the shell gap between the neutron $d_{3/2}$ and the pf orbitals is reduced by about 1 MeV for the Mg isotone and about 2 MeV for the Ne isotone

[9]. Thus, excitations of 2p2h intruder configurations of *sd* and *pf* orbitals are increased for the neutron-rich Ne, Na, and Mg isotopes. The intruder configurations gain correlation energy, i.e., deformation energy, comprising proton-neutron and neutron-neutron monopole and quadrupole terms [10]. If this gain of correlation energy largely compensates the loss of energy promoting two neutrons from the $d_{5/2}$ orbital across the $N = 20$ shell gap to a *pf* orbital ($2E_{\mathrm{gap}}$), the ground-state wave function contains a dominant 2p2h admixture. Thus, normal (0p0h) and intruder (2p2h) configurations are inverted in those nuclei at the island of inversion. Moreover, due to deformation of the ground state, nuclei which reside in the region of the island of inversion, show largely collective behavior, e.g., reduced $E(2^+)$ and increased $B(E2,0^+ \rightarrow 2^+)$ values for even-even isotopes. In addition to the shell-model calculations, the low-lying 2_1^+ states and increased $B(E2)$ values were reproduced also by the quasiparticle random-phase approximation [11] and configuration mixing with angular-momentum projection [12,13]. Mean-field calculations result in a spherical shape for the ground state of ^{32}Mg [14,15]. However, it is calculated to be very soft against quadrupole deformation.

A number of experimental and theoretical studies have been carried out in order to understand the coexistence of normal 0p0h and intruder 1p1h and 2p2h configurations at low energies for different isotopes in the region of the island of inversion. However, the driving mechanisms are not fully understood yet and the predictive power of most theories is not good enough to provide reliable information on the low-energy structure and experimental observables for many nuclei in this region. Detailed theoretical information is rare, especially for nuclei with odd N and/or odd Z, although these nuclei are a sensitive probe for the competing structure of 0p0h, 1p1h, and 2p2h configurations at low energies.

In the neutron-rich Mg isotopes with $N = 20$–22, the inverted level structure of normal and intruder configurations at low energies has been firmly established in a series of experiments [16–20]. More recently it could be confirmed that already at $N = 19$ the wave functions of the ground and low-lying states contain a dominant admixture of intruder configurations [21–23]. For the neighboring $N = 18,19$ Na isotopes, ^{29,30}Na, measurements of the magnetic dipole moments and electric quadrupole moments revealed significant deviations from the universal *sd*-shell (USD) model [24,25], indicating a dramatic change in the underlying shell structure also for these nuclei.

While the experimentally deduced magnetic dipole moment of ^{29}Na could be reproduced in USD calculations, its electric quadrupole moment exceeded the USD value by about 30% [25,26]. Monte Carlo shell model (MCSM) calculations with the SDPF-M interaction reproduced this anomalous electric quadrupole moment, as well as the close-lying ground and first excited states with spin values $3/2^+$ and $5/2^+$, observed in β-decay studies [27,28], supposing a large mixing of intruder configurations by about 42% for the wave function of the ground state [26]. Moreover, the MCSM calculation yields an $E2$ excitation strength of the low-lying states with $B(E2,3/2^+ \rightarrow 5/2^+) = 135\ e^2\mathrm{fm}^4$, compared to 111 $e^2\mathrm{fm}^4$ obtained by the USD model. Results of a recently published

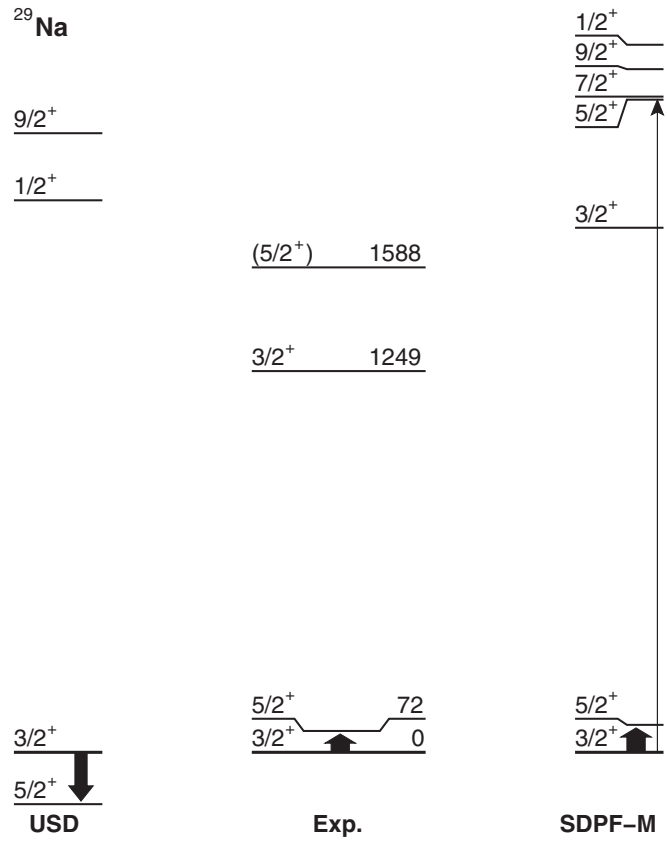

FIG. 1. Comparison of the energy levels of ^{29}Na, deduced by experiment (middle) and by shell-model calculations using the USD (left) and SDPF-M interactions (right). The $E2$ excitation strengths from the ground state are indicated by the width of the arrows. The figure was adapted from Refs. [26–28].

Coulomb-excitation experiment favored the former value with $B(E2)\uparrow = 140(25)\ e^2\mathrm{fm}^4$ [29]. Other low-lying states are supposed to be dominated by normal 0p0h configurations and are hardly connected to the ground state. Thus, very small $B(E2)$ values are expected. Utsuno *et al.* predicted higher-lying $3/2_2^+$, $5/2_2^+$, and $7/2_1^+$ states dominated by intruder configurations at around 2 MeV [26] (cf. Fig. 1). New β-decay studies assigned states at 1249 and 1588 keV to have $J^\pi = 3/2_2^+$ and $(5/2_2^+)$, respectively [28]. Additional MCSM calculations obtained 65% and 77% 2p2h admixture for the $3/2_2^+$ state and $5/2_2^+$ state, respectively [28]. Due to the large intruder mixing in the ground state these states are supposed to have a noticeable overlap with the ground state in their wave functions. Thus, the related $B(E2)$ values are sensitive probes related to the intruder content and the $N = 20$ shell gap. A value of $B(E2,3/2_{\mathrm{gs}}^+ \rightarrow 7/2_2^+) = 57\ e^2\mathrm{fm}^4$ has been reported [26] and is awaiting experimental verification.

The magnetic dipole moment of ^{30}Na was experimentally deduced by Keim *et al.* to be 2.069(2) μ_N^2, which is significantly lower than the predicted value from USD model calculations, which yielded $\mu = 2.687\ \mu_N^2$ [25]. Moreover, an anomalous electric quadrupole moment was measured [24,30]. Its value and also its sign differ markedly from the USD prediction. MCSM calculations with the SDPF-M interaction

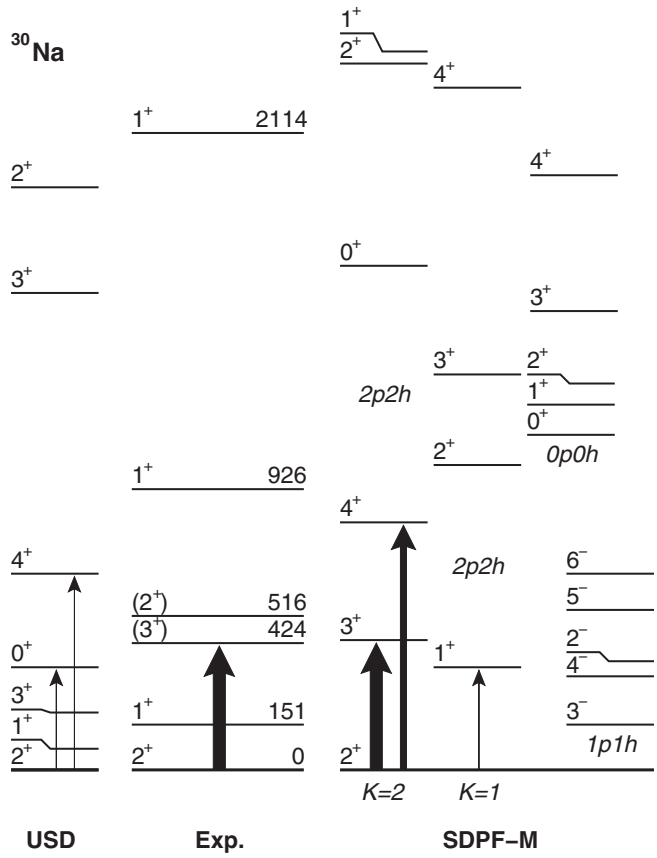

FIG. 2. Comparison of the energy levels of ^{30}Na, deduced by experiment (middle) and by shell-model calculations using the USD (left) and SDPF-M interactions (right). The $E2$ excitation strengths from the ground state are indicated by the width of the arrows. The figure was adapted from Refs. [26–28].

reproduced the measured μ and Q_0 values very well [26]. Thus, the properties of the electromagnetic moments indicate that already at $N = 19$ the ground state in ^{30}Na is dominated by intruder configurations. A rotational $K = 2$ band was obtained by the MCSM calculations, built upon the 2^+ ground state (cf. Fig. 2), characterized by highly collective $E2$ intraband transitions. The reduced transition probabilities amounted to a $B(E2,2_1^+ \rightarrow 3_1^+) = 168\ e^2\text{fm}^4$ and $B(E2,2_1^+ \rightarrow 4_1^+) = 90\ e^2\text{fm}^4$ [26]. To probe these values intermediate-energy Coulomb-excitation experiments of ^{30}Na were performed. Values of $E_\gamma = 433(16)$ keV with $B(E2)\uparrow = 130^{+90}_{-65}\ e^2\text{fm}^4$ were published by Pritychenko *et al.* [30] and confirmed very recently by Ettenauer *et al.*, who measured $E_\gamma = 424(3)$ keV and $B(E2)\uparrow = 147(21)\ e^2\text{fm}^4$ [31]. Both results agree well with the predicted decay of the first excited 3_1^+ state. Collective transitions of higher-lying states were not observed. In the particle-rotor model the strong prolate deformation of ^{30}Na can be described with an intrinsic state, which couples the deformed ^{28}Ne rotor with a proton in the $\pi[211]3/2^+$ Nilsson orbital and a neutron in the $\nu[200]1/2^+$ orbital, allowing for a $K = 1$ or $K = 2$ yrast band. The MCSM calculations predicted the $K = 2$ band to be energetically favored with respect to the $K = 1$ band [26], which is consistent with the measured ground-state spin. The $K = 1$ bandhead was calculated at 0.31 MeV and its $J = 2$ and 3 members at around 1 MeV excitation energy (cf. Fig. 2). A promising candidate for the $K = 1$ bandhead was found by a new β-decay experiment, which observed a 1^+ state at 150 keV [28]. States, dominated by normal, spherical 0p0h configurations, were expected at around 1–1.5 MeV. Moreover, the MCSM calculations predicted rather low-lying negative-parity states, which were dominated by 1p1h excitations across the $N = 20$ shell gap [26]. Thus, in ^{30}Na normal and intruder configurations were supposed to compete with each other at low excitation energies. Detailed experimental studies of these states would reveal excellent information on the underlying shell-model modifications around $N = 20$.

To probe the predicted collective properties of the first and higher-lying excited states in ^{29,30}Na, Coulomb-excitation experiments in inverse kinematics were proposed at REX-ISOLDE, CERN, employing postaccelerated radioactive ^{29,30}Na beams at "safe" energies, i.e., the distance of closest approach is >15 fm and the contribution of nuclear interaction to the total excitation cross section is <0.1% [32]. The intruder configurations also at higher excitation energy were a subject of these experiments to obtain new information about the underlying shell structure and the evolution of the shell gaps far from stability. Compared to the results published by Hurst *et al.* [29] and Ettenauer *et al.* [31], the presented experiments should benefit from the more intense radioactive ion beams at REX-ISOLDE, a reduced background at energies below 250 keV and the high energy resolution and detection efficiency of the MINIBALL setup.

II. EXPERIMENTAL SETUP AND DATA ANALYSIS

The Coulomb-excitation experiments of ^{29,30}Na were performed at the REX-ISOLDE facility at CERN [33,34]. The short-lived radioactive ^{29,30}Na beams (half-lives $T_{1/2} = 44.9(12)$ ms (^{29}Na) [35] and $T_{1/2} = 48(2)$ ms (^{30}Na) [36]) were produced by bombarding an approximately 50-g/cm^2-thick UC_x target with 1.4-GeV protons, provided by the CERN PS Booster, with a maximum intensity of 3.2×10^{13} p/pulse. The pulses were spaced in time by integer multiples of 1.2 s, allowing for an average proton current of 2 μA. The produced Na ions were surface ionized on a tungsten surface and were mass separated by the ISOLDE High Resolution Separator (HRS). The ion beam was then guided to REX-ISOLDE, where the ions were first accumulated, cooled, and bunched in a Penning trap before injecting into an Electron Beam Ion Source (EBIS) [37]. In the REXEBIS the ions were charge bred to high charge states. Due to the very short half-lives of the isotopes, special attention had to be paid on the optimization of the working cycle of the REX-ISOLDE charge breeding system in order to minimize losses caused by in-trap decay. Therefore the trap accumulation and charge breeding times were set to 20 and 13 ms, respectively. After an A/q separation with $A/q = 4.143$ for ^{29}Na and $A/q = 4.286$ for ^{30}Na (both $q = 7+$) the radioactive beam was postaccelerated by the REX linear accelerator and delivered with a final beam energy of 2.85 MeV/nucleon onto the secondary target inside the highly-efficient MINIBALL setup [38]. The average intensities of the

postaccelerated ion beams amounted to 2700(100) ions/s and 650(250) ions/s for ^{29}Na and ^{30}Na, respectively. During the Coulomb-excitation experiments two enriched ^{104}Pd and ^{120}Sn targets were used with effective thicknesses of 4.1 mg/cm^2 and 4.0 mg/cm^2, respectively. The ^{104}Pd target was a stack of two targets (2.2 mg/cm^2 and 1.9 mg/cm^2). The beam-on-target times added up to 64 h for the ^{29}Na beam and 84 h for the ^{30}Na beam.

The scattered beam nuclei were detected by a CD-shaped, 500-μm-thick, double-sided silicon strip detector (DSSSD), consisting of four identical quadrants [38,39]. Each quadrant comprised 16 annular strips at the front side and 12 pairs of sector strips at the back side for identification and reconstruction of the trajectories of the scattered nuclei. Calibration of all DSSSD segments was done with an α source, containing ^{239}Pu, ^{241}Am, and ^{244}Cm. The detector covered forward angles between 16.8° and 53.7° in the laboratory system. De-excitation γ rays following Coulomb excitation of projectile and target nuclei were detected by the MINIBALL γ-ray spectrometer, consisting of eight triple cluster detectors in close geometry, each containing three sixfold segmented HPGe crystals [38,40]. To calibrate the MINIBALL clusters and to determine their individual, energy-dependent efficiency down to 50 keV, ^{60}Co, ^{133}Ba, and ^{152}Eu sources were mounted onto the target frame at target position. The total photopeak efficiency of the array at 1.3 MeV was 8.4(2)% after the addback procedure was applied, i.e., coincident signals of the three detectors of a MINIBALL cluster were combined. At low γ-ray energies around 81 keV the photopeak efficiency amounted still 23.8(4)%. For Doppler correction, all angles of the cluster detectors had to be known exactly. Therefore an angle-calibration measurement was performed, using Doppler-shifted γ rays after the neutron pick-up reaction $d(^{22}\mathrm{Ne}, ^{23}\mathrm{Ne})p$. The high segmentation of the setup ensured a proper Doppler correction for in-flight γ-ray emission at $v/c \sim 8\%$ by combining the angular information of the γ ray with the direction and velocity of the scattered beam particle that was detected in coincidence. Data of the Coulomb-excitation measurements were recorded using prompt particle-γ coincidences, i.e., events with a maximum time difference of typically 800 ns between particle and γ ray were registered.

In Coulomb-excitation experiments with radioactive beams, possible beam contaminations have to be carefully investigated, because all beam components contribute to Coulomb excitation of the target material, which is used for normalization. For the extraction of the transition probabilities it was mandatory to monitor and to determine the exact beam composition during the experiment, using two different techniques. First, the time dependence of the RIB intensity with respect to the proton-beam impact on the primary ISOLDE target was analyzed as shown in Fig. 3. Due to their fast release out of the primary target [41] and their short lifetimes the ^{29}Na and ^{30}Na ions showed a high intensity only for the first ~280 ms after the proton pulse. For longer times longer-lived contaminants, in particular isobaric Al and Mg isotopes, dominated the beam composition. By setting an appropriate time gate, the amount of beam contaminants could be reduced by a factor of 6.5 and 4.3 for the ^{29}Na and ^{30}Na data, respectively. In a second step the exact beam composition was

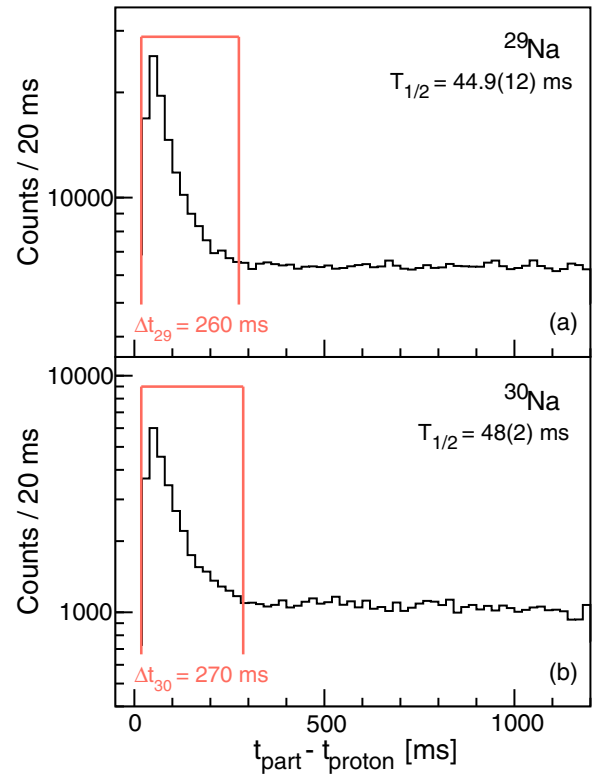

FIG. 3. (Color online) Time-dependent intensity of $A = 29,30$ ions, scattered into the DSSSD, with respect to the last proton beam impact onto the ISOLDE target for the ^{29,30}Na runs. The time gates Δt_A set to select the short-lived Na isotopes and to reduce the amount of beam contaminants in the analysis are indicated in red.

determined with help of an ionization chamber, consisting of a gas cell and a Si detector in succession for the ΔE_{gas} and E_{res} measurements, respectively, which was mounted downstream after the scattering chamber at the beam-dump position (see Fig. 4).

For the $A = 29$ beam the accumulated radioactive beam composition of the experiment amounted to 29.5(7)% for ^{29}Na within a time window of 260 ms after the proton pulse impact, which was applied in the further analysis of the measured γ-ray intensities. Other beam fractions were found to be 12.1(3)% for ^{29}Mg, 57.7(9)% for ^{29}Al, and 0.7(1)% for ^{29}Si. For the $A = 30$ beam the accumulated radioactive beam composition of the experiment amounted to 47.3(21)% for ^{30}Na within a time window of 270 ms after the proton pulse impact. Other beam fractions were found to be 13.6(9)% for ^{30}Mg, 38.5(19)% for ^{30}Al, and 0.6(2)% for ^{30}Si.

Coulomb-excitation data analysis commenced by selecting scattered projectile nuclei, i.e., ^{29,30}Na, which were detected by the DSSSD. The kinematics of the scattered beam or target nuclei is clearly separated by the measured correlation of particle energy and scattering angle. A time window with a width of typically $\Delta t_p \sim 145$ ns was applied on the time difference between the particle and the γ ray to select the prompt Coulomb-excitation events and to suppress random coincidences from room background, i.e., β decay and bremsstrahlung. The prompt Coulomb-excitation spectrum for

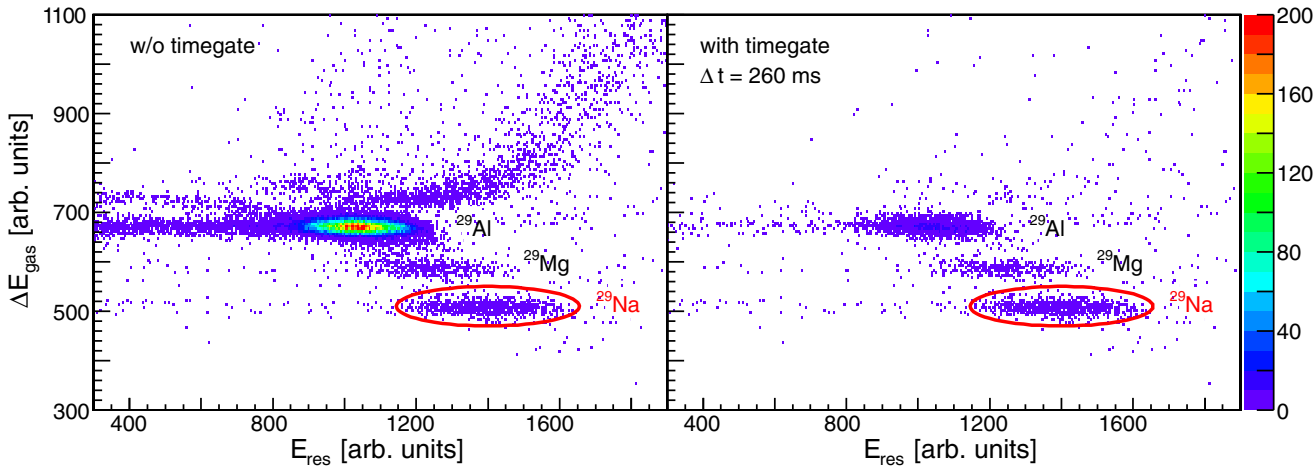

FIG. 4. (Color online) ΔE_{gas}-E_{res} spectra of the beam composition, taken with the ionization chamber during the ^{29}Na beam time. The $A = 29$ isobars are well separated and can be clearly identified. While for the left spectrum no time gate is applied, the right spectrum contains only those ions, which arrive at the ionization chamber within the first 260 ms after the proton pulse impact. A significant reduction of beam contaminants is achieved, in particular for ^{29}Al, while the number of ^{29}Na ions remains constant. More information is given in the text.

the further analysis is particularly clean of any background transitions after background subtraction with a long time window $\Delta t_r \sim 1450$ ns. All observed γ-ray transitions are due to Coulomb excitation of either beam or target nuclei.

III. RESULTS

A. Coulomb excitation of ^{29}Na

Scattered ^{29}Na ions were selected by a particle gate on the measured correlation of particle energy and scattering angle in the DSSSD. Using the energy and position information of the scattered particle and the coincident γ ray, which were provided by the segmentation of the DSSSD and the MINIBALL detectors, respectively, a proper Doppler correction of the emitted γ rays was performed. For the projectile, Doppler correction is essential due to the relatively high recoil velocities $\beta > 5\%$. The resulting prompt, background-subtracted γ-ray spectra are shown in Fig. 5. Deexcitation γ rays of excited states of both projectile and target nuclei were observed. The well-known $2^+ \rightarrow 0^+$ transition in ^{104}Pd at 555.8 keV [42] was the strongest γ-ray transition in the spectrum. Another γ-ray transition was observed in the spectra at 72 keV, which was assigned to the depopulation of the proposed $5/2^+$ state in ^{29}Na, already known from β-decay studies [43]. At this low γ-ray energy, special attention had to be paid to the background radiation, especially strong x-ray radiation following β decay of long-lived decay products of ^{200}Po, studied at the MINIBALL setup prior to the Coulomb-excitation experiment on the neutron-rich Na isotopes, interfering with the 72-keV transition of ^{29}Na.

MCSM calculations by Utsuno *et al.* predicted γ-ray transitions depopulating deformed $3/2^+_2$, $5/2^+_2$, and $7/2^+_1$ states in ^{29}Na at around 2 MeV, which could be excited with a moderately large excitation strength [26]. For instance, a possible $7/2^+_1$ state is predicted to be excited with a transition strength of $B(E2,3/2^+_1 \rightarrow 7/2^+_1) = 57\ e^2\text{fm}^4$ [26]. No clear experimental sign was found for such transitions in the range of 1500–2400 keV, due to the low count rate and insufficient statistical significance, i.e., fewer than three counts (cf. Fig. 5). The most promising candidate at 1518(4) keV was already known from β-decay studies as depopulating transition of a $(5/2^+_2)$ state at 1588 keV [43].

The unknown reduced transition probabilities of excited states of ^{29}Na were determined using the relative deexcitation γ-ray yields between ^{29}Na and the Coulomb excited, well-known 2^+ state of ^{104}Pd. The deexcitation yield of the 555.8-keV transition of ^{104}Pd was corrected with the deduced effective beam composition, including the different Coulomb-excitation cross sections of the isobars for excitation of the target material, yielding a ^{29}Na fraction of 32.2(10)% for the excitation of the 2^+ state. To fit the electromagnetic transition matrix elements to the experimental data, the coupled-channels Coulomb-excitation code GOSIA [44,45] was used. The calculations were performed by integrating over the scattering angle range of $\Theta_{\text{c.m.}} = 20.9$–$66.2^\circ$, which is covered by the DSSSD, and the energy loss of the projectile in the target material. Corrections of the measured γ-ray yields for angular distribution effects and internal conversion were taken into account as well as position and relative efficiency of the MINIBALL cluster detectors.

The spin and parity of the 72-keV level were determined to be $J^\pi = 5/2^+$ [28], in agreement with MCSM calculations which favor a $5/2^+$ above the $3/2^+$ ground state [26]. The spectroscopic quadrupole moment of the ground state was measured by β-nuclear magnetic resonance (NMR) spectroscopy, yielding a value of $Q_{3/2^+} = +0.086(3)\ e$b[25]. This quadrupole moment was included in the calculations as diagonal matrix element $\langle 3/2^+||E2||3/2^+\rangle$. For the 72-keV level the diagonal matrix element was assumed to be $|\langle 5/2^+||E2||5/2^+\rangle| = 0.039(3)\ e$b within a rotational model with $K = 3/2$.

Including this information, the GOSIA calculations yielded a reduced transition probability of $B(E2,3/2^+ \rightarrow 5/2^+) = 150(20)\ e^2\text{fm}^4$ for the Coulomb excitation of the $5/2^+$ state at

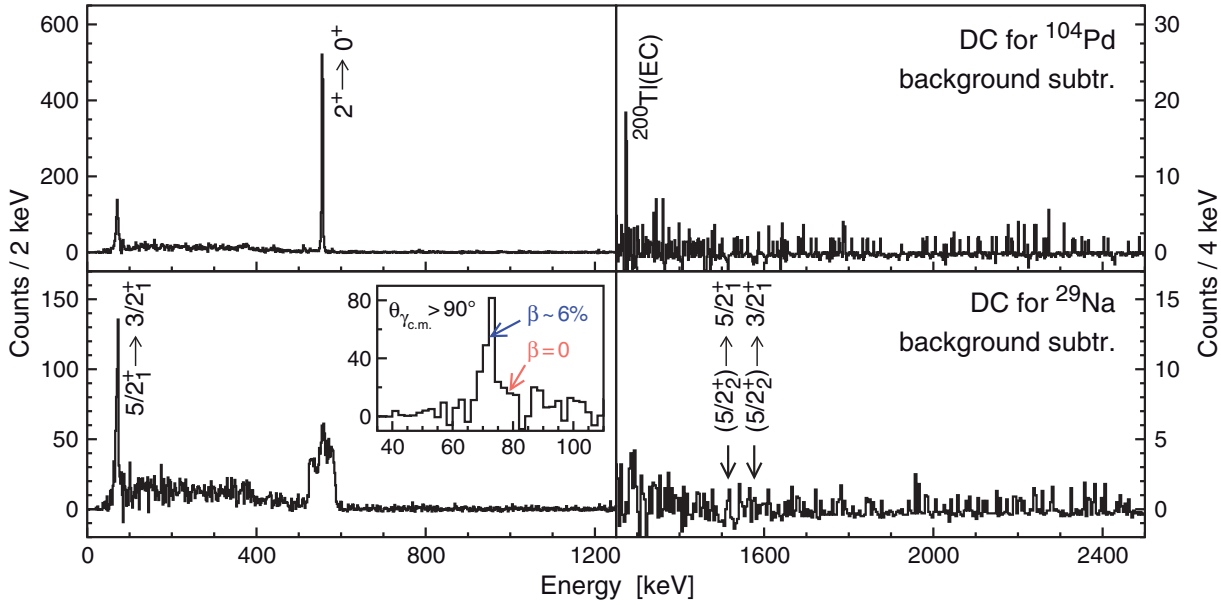

FIG. 5. (Color online) Doppler-corrected and background-subtracted γ-ray spectra of the Coulomb excitation of ^{29}Na in coincidence with scattered beam particles. Doppler correction (DC) was performed for the ^{104}Pd target (top) and ^{29}Na beam (bottom). γ-ray transitions from the Coulomb excitation of ^{29}Na and ^{104}Pd nuclei were detected. The sharp line at 1275 keV is artificial from ^{200}Tl EC decay. Please note the different scaling on the y axis. The inset for the low-energy spectrum of ^{29}Na shows the line shape of the 72-keV transition detected in backward direction, with the properly Doppler-corrected γ-ray events emitted in flight ($\beta \sim 6\%$). For ^{29}Na ions implanted in the DSSSD the γ rays would be wrongly Doppler corrected ($\beta = 0$).

72 keV. The quoted error is dominated by the statistical error of almost 10% for the measured γ-ray yield but also includes a 6% error for the correction for the x-ray radiation background and a 5% error for unobserved feeding from higher-lying excited states. Uncertainties of the beam composition and target excitation were included with 3% and 2%, respectively. The obtained value agrees very well with the transition strength of $B(E2)\uparrow = 140(26)\ e^2\text{fm}^4$, which was published by Hurst *et al.* [29].

The average time-of-flight of the scattered $A = 29$ ions between target and DSSSD was 2.0 ns. Most of the γ rays were detected with a certain Doppler shift, indicating a dominant in-flight decay. Thus, the lifetime of the 72-keV level has to be significantly shorter than the average time-of-flight. An upper limit of 1.5 ns was assumed from the measured spectrum. To reproduce the observed lifetime limit, deexcitation of the 72-keV level has to proceed via a strong $M1$ transition. The GOSIA calculations yielded a lower limit of $B(M1,5/2^+ \rightarrow 3/2^+) > 0.06\ \mu_N^2$ for the $M1$ strength. This corresponds to a multipole mixing ratio $|\delta| < 0.025$.

An upper limit can be calculated for the excitation of the 1588-keV state, known from β-decay studies [28,43]. Spin and parity of this state are assigned to $1/2^+$, $3/2^+$, or $5/2^+$ due to the measured log $ft = 4.64$ value in combination with the $3/2^+$ ground state of ^{29}Ne [28,35]. However, the calculated excitation strength varies only marginally (~5%) with the assumed spin value of the 1588-keV state, yielding $B(E2,3/2^+ \rightarrow (5/2^+_2)) < 70\ e^2\text{fm}^4$. For the proposed $7/2^+$ state [26], as well as for any other higher-lying excited state in ^{29}Na, only an upper limit could be given for the reduced transition probability. Therefore a detection limit of 2.5 counts was assumed for a transition on an average background of almost 0.1 counts/keV, measured in this experiment with the MINIBALL setup in the energy range between 1600 and 2500 keV. It was assumed that the $7/2^+$ state had to decay to the $5/2^+$ state at 72 keV with a branching ratio of almost 100%. Any other branching, e.g., the direct decay into the ground state, was neglected. To reproduce the measured γ-ray yields the $E2$ excitation strength of the $3/2^+ \rightarrow 7/2^+$ transition has to be smaller than the upper limit indicated by the solid line in Fig. 6. Thus, an excitation to a $7/2^+$ state

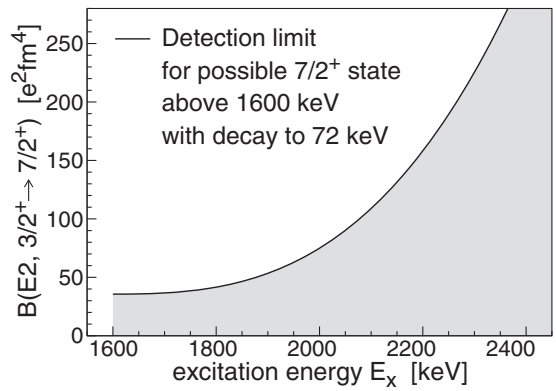

FIG. 6. Calculated upper limit for the excitation strength of a possible $3/2^+ \rightarrow 7/2^+$ transition in ^{29}Na between 1600 and 2450 keV (solid line) in the present experiment in order to reproduce the measured γ-ray yields. Detailed information is given in the text.

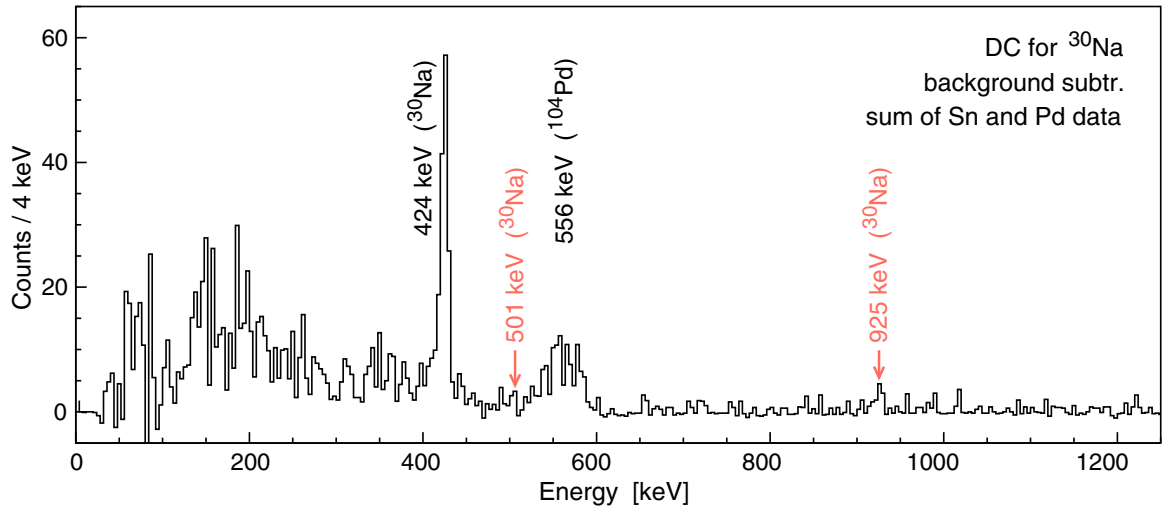

FIG. 7. (Color online) Sum spectrum of the Coulomb-excitation experiments on ^{30}Na, using the data sets taken with the ^{104}Pd target and the ^{120}Sn target, background subtracted and Doppler corrected (DC) for ^{30}Na. In addition to the known 424-keV transition there is evidence for two weak transitions at 925(4) keV and 501(4) keV (arrows), depopulating an excited state at 925(5) keV. Events with 511 keV coming from background radiation were suppressed.

below 1900 keV would have to have a $B(E2)$ value similar to or even smaller than the predicted 57 e^2fm^4 [26], whereas a higher-lying $7/2^+$ state with such a $B(E2)$ value could not be detected at all in the present experiment. A $7/2^+$ state at around 2300 keV would need to be connected to the ground state with $B(E2)\uparrow \approx 230\ e^2\text{fm}^4$, to be detected with 2.5 counts.

B. Coulomb excitation of ^{30}Na

In addition to the ^{29}Na experiment, another Coulomb-excitation experiment in inverse kinematics on the neighboring $N = 19$ isotope ^{30}Na was carried out to further study the expected transition from spherical sd shell to deformed sd-pf shell configurations at the island of inversion. As in the ^{29}Na experiment, scattered ^{30}Na nuclei were selected by means of the measured correlation between scattering angle θ_{CD} and energy deposited in the DSSSD. Figure 7 shows the resulting Doppler-corrected and background-subtracted γ-ray spectra of the two parts of the experiment, employing the ^{120}Sn and ^{104}Pd target. In order to facilitate observation and identification of weak γ-ray transitions in ^{30}Na, data sets taken with both targets, i.e., ^{120}Sn and ^{104}Pd, were summed.

γ-ray transitions, depopulating excited states, were observed for both target and projectile nuclei. Doppler correction for scattered $A = 30$ projectiles revealed a strong γ-ray transition at 424 keV, which was already observed in a previous Coulomb-excitation experiment of ^{30}Na by Ettenauer *et al.* [31]. These γ-ray events were assigned to the deexcitation of a (3^+) state at 424 keV to the 2^+ ground state. Deexciting transitions of low-lying excited 1^+ states, which were known from β-decay studies of ^{30}Ne [28], were not observed in this Coulomb-excitation experiment. An accumulation of γ-ray events at around 925(4) keV could be interpreted as a possible candidate for the deexcitation of a proposed (4^+) state in ^{30}Na (cf. Fig. 9). MCSM calculations predicted a strong $4^+ \rightarrow 3^+$ transition with $B(M1,4^+ \rightarrow 3^+) = 0.43\ \mu_N^2$ [31]. Thus, an additional branching to the (3^+) state with a transition energy of 501(4) keV should be observed. With the high γ-ray efficiency of the MINIBALL array a verification of this prediction should be feasible by the measured coincidence relations. Taking into account the measured yields in the γ-ray singles spectrum and the γ-ray efficiency of the MINIBALL array, one detected event with coincident 501-keV and 424-keV γ rays could be expected. Experimental data—taken with both targets (Sn and Pd)—were sorted into a prompt particle-$\gamma\gamma$ coincidence matrix. Coincidence gates were set on the $(3^+) \rightarrow 2^+$ transition at 424 keV and on the proposed $(4^+) \rightarrow (3^+)$ transition at 501 keV to investigate γ-ray transitions feeding the (3^+) state. The cut spectrum showed γ-ray events at 501 and 424 keV, respectively, as shown in Fig. 8. This would be perfectly in line with the results deduced from the γ-ray singles spectra, which favored an excited state at 925(5) keV with about 67(10)% γ-ray decay branching to the 2^+ ground state and about 33(10)% branching to the (3^+) state at 424 keV. This state at 925 keV is a possible candidate for the proposed 4^+ state in ^{30}Na [26]. The known decay branches of the nearby 1_2^+ state at 926(2) keV, which was observed by β-decay studies [28], were not observed in the present Coulomb-excitation experiment.

The reduced excitation probabilities of the excited states in ^{30}Na, which are of further interest, were determined by means of the measured intensities of the depopulating γ-ray transitions, relative to the well-known cross section for the Coulomb excitation of the target nuclei. The electromagnetic transition matrix elements were fitted using the GOSIA code [44,45]. The spin and parity of the 424-keV level in ^{30}Na are not fixed experimentally, but recent shell-model calculations favored a deformed 3^+ state at this energy [26,31]. Furthermore, shell-model calculations favored a deformed 4^+ state at around 800 keV [26], which could be assigned to the newly observed 925-keV state. The quadrupole moment of the 2^+ ground state was predicted to be $Q(2^+) = 16\ e$fm

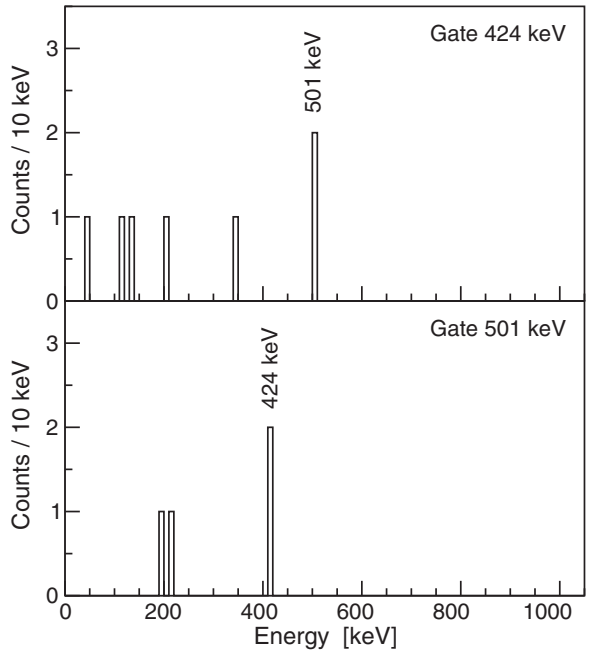

FIG. 8. Prompt particle-$\gamma\gamma$ coincidence spectrum of the Coulomb excitation of ^{30}Na, gated on the 424-keV transition (top) and on the newly observed 501-keV transition (bottom), for the sum of both targets (Sn and Pd). Coincident γ-ray transitions were observed at 501 keV, feeding the 424-keV level. Doppler correction was performed for the detected ^{30}Na nucleus. γ rays with a detected energy between 508 and 514 keV were excluded from the analysis to eliminate random coincidences with 511-keV γ rays.

[26]. Within a rotational model applied to the $K = 2$ yrast band, values for the diagonal matrix elements were included in the GOSIA calculations. Predictions within the MCSM expect a rather large $M1$ contribution for the $2^+ \rightarrow 3^+$ transition with a transition strength of $B(M1)\uparrow = 0.268\ \mu_N^2$ [31]. All additional information on low-lying levels up to 1 MeV, e.g., energy, spin, parity, branching ratio, etc., which were determined by β-decay studies [28], was taken into account.

For the excitation of the 424-keV level in ^{30}Na the GOSIA calculations yielded excitation strengths of $B(E2,2^+ \rightarrow (3^+)) = 230(40)\ e^2\text{fm}^4$ and $B(E2,2^+ \rightarrow (3^+)) = 320(100)\ e^2\text{fm}^4$ for the measurement with the ^{104}Pd and ^{120}Sn target, respectively. Furthermore, the possible (4^+) state at 925 keV was calculated to be populated with a value of $B(E2,2^+ \rightarrow (4^+)) = 125(45)\ e^2\text{fm}^4$ and $B(E2,2^+ \rightarrow (4^+)) = 96(50)\ e^2\text{fm}^4$ for the two different targets. Deexcitation of the (4^+) state had to proceed via an $E2$ transition to the ground state, competing with a mixed $E2+M1$ transition to the (3^+) state. To reproduce the measured branching ratios the $M1$ component of the $(4^+) \rightarrow (3^+)$ transition had to be much smaller than the value of $0.43\ \mu_N^2$, predicted by MCSM calculations [31]. Assuming a moderate $E2$ strength of $B(E2) = 80\ e^2\text{fm}^4$ for the 501 keV transition, the GOSIA calculation yielded a $M1$ strength of $B(M1,(4^+) \rightarrow (3^+)) = 0.027(14)\ \mu_N^2$. All quoted errors are mainly dominated by the statistical errors of the measured deexcitation yields of the relevant projectile and target excitations, respectively. Systematic errors arising from uncertainties of the deduced beam composition and of the calculated target excitation cross section were minor and were taken into account with about 5% and 3%, respectively.

IV. DISCUSSION

A. ^{29}Na

The measured reduced transition probabilities of the $N = 18$ nucleus ^{29}Na are compared to recently published experimental values [29] and MCSM predictions [26]. The transition strength of the $5/2_1^+ \rightarrow 3/2^+$ transition at 72 keV deduced in this work yielded $B(E2,3/2^+ \rightarrow 5/2_1^+) = 150(20)\ e^2\text{fm}^4$. This value is in good agreement with the value of $B(E2)\uparrow = 140(25)\ e^2\text{fm}^4$ published by Hurst and collaborators [29]. Recent shell-model calculations using the USD interaction and the SDPF-M interaction predict an excitation strength of 111 and 135 $e^2\text{fm}^4$, respectively, for the $5/2_1^+$ state [26]. Thus, the experimental results are consistent with the predictions by the MCSM calculations using the SDPF-M interaction, which yielded a mixing of intruder configurations by 42% and 32% for the wave function of the $3/2^+$ ground state and the first excited $5/2_1^+$ state, respectively [26,28], confirming the onset of large intruder admixtures in the ground-state wave function already for the $N = 18$ isotope ^{29}Na. Within a simple rotational model the measured transition strengths yielded $Q_0 = 0.542(36)\ e\text{b}$ for the intrinsic electric quadrupole moment of the ground state of ^{29}Na, assuming a prolate deformation. This gives a quadrupole deformation parameter of $\beta_2 = 0.48(3)$, using the equation given in Ref. [46]. However, this simple model overestimates the quadrupole deformation of ^{29}Na due to the different static and dynamic nuclear properties, arising from differences in the underlying single-particle configurations of the ground and first excited states. An earlier, precise β-NMR measurement pointed to slightly less deformation: $Q_0 = 0.430(15)\ e\text{b}$ and $\beta_2 = 0.38(2)$ [25].

To further investigate the mechanism of intrusion in the neutron-rich Na isotopes, the experiment searched for collective properties of possible higher-lying $3/2_2^+$, $5/2_2^+$, and $7/2_1^+$ states dominated by intruder configuration, which were predicted by MCSM calculations [26]. A possible candidate for a weak transition might be observed at 1518(4) keV, de-exciting a known level at 1588 keV, which was assigned as $(5/2_2^+)$ state by new β-decay studies [28]. An upper limit for the reduced transition probability was deduced, yielding $B(E2,3/2^+ \rightarrow (5/2_2^+)) < 70\ e^2\text{fm}^4$. This value is consistent with the moderately large $B(E2)\uparrow$ values predicted by theory for the intruder dominated states around 1.5–2.5 MeV [26]. Additionally, the measured $B(E2)$ value implies a large 2p2h admixture in the wave function of the 1588-keV state and a significant coupling to the ground state due to the large intruder mixing. Indeed MCSM calculations predicted 77% intruder admixture for the $5/2_2^+$ state [28]. Other transitions of intruder-dominated higher-lying states predicted by theory were not observed. However, conclusive results of transition probabilities of higher-lying deformed states were not possible due to the experimental limitation and low count rates.

TABLE I. Experimentally deduced reduced transition probabilities of the positive-parity $K = 2$ ground-state band in ^{30}Na, compared to recent theoretical predictions by MCSM calculations. The first two columns represent the results of the presented experiments using the two different scattering targets (^{104}Pd and ^{120}Sn). $B(E2)$ values are given in e^2fm^4, $B(M1)$ in μ_N^2. Details are given in the text.

	$B(E2)$				$B(M1)$	
$I_i \rightarrow I_f$	(Pd target)	(Sn target)	(previous exp.)	(MCSM)	(Pd target)	(MCSM)
$2^+_{gs} \rightarrow 3^+$	230(41)	320(100)	147(21)[a]	168[b]		0.268[a]
$2^+_{gs} \rightarrow 4^+$	125(45)	96(50)		90[b]	–	–
$4^+ \rightarrow 3^+$					0.027(14)	0.43[a]

[a]From Ref. [31].
[b]From Ref. [26].

B. ^{30}Na

The measured level scheme and reduced transition probabilities of ^{30}Na are compared to results from recently published experimental studies [28,31,47] and different shell-model predictions [26]. The excited state at 424 keV was already established in previous Coulomb-excitation experiments [30,31] and proton inelastic-scattering studies of ^{30}Na [47] to be the $J = 3$ member of the $K = 2$ rotational band built upon the 2^+ ground state. This result fits perfectly with MCSM calculations using the SDPF-M interaction, which predicted the $J = 3$ state at 430 keV excitation energy [26]. Moreover, theory predicted the $J = 4$ member of the $K = 2$ rotational band at an excitation energy of around 860 keV. The newly observed γ-ray transitions at 501(4) keV and 925(4) keV were proposed to be deexciting transitions of a level at 925(4) keV by coincidence relations. Coulomb-excitation relations prefer $J^\pi = (4^+)$ for this state in agreement with the MCSM predictions (see Fig. 9). However, this state and its γ-ray decay were not observed in the previous Coulomb-excitation experiments [30,31]. γ-ray events deexciting the $K = 1$ band head at 151 keV, known as strongest γ-ray transition in β-decay studies of ^{30}Na [28], were not observed. Thus, only an upper limit for the excitation of the 1^+_1 state with $B(E2)\uparrow < 25$ e^2fm^4 could be deduced, indicating a reduced coupling of the $K = 1$ band to the $K = 2$ ground-state band. This would support the results of a proton inelastic scattering experiment on ^{30,31}Na, assuming different proton configurations of the $K = 1$ and $K = 2$ band members [47].

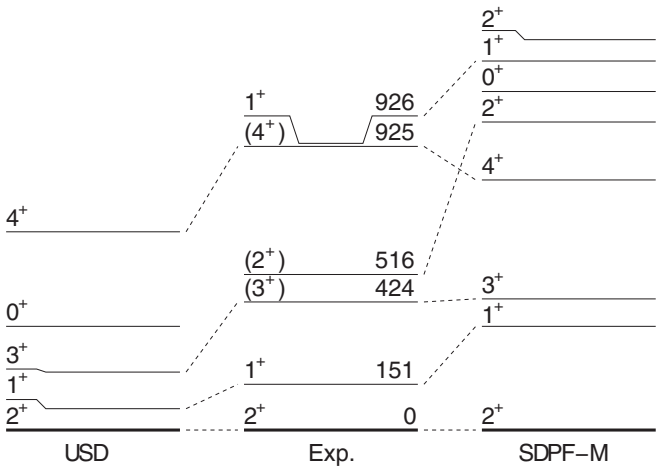

FIG. 9. Level scheme of ^{30}Na, as it was extracted from the present Coulomb excitation and previous β-decay data [28] (middle), compared to recently published MCSM calculations [26] using the SDPF-M interaction (right) and the USD interaction (left). Excitation energies are given in keV.

The observed collective properties of excited states in ^{30}Na are in agreement with intruder-dominated configurations, predicted by recent theoretical approaches [26] (see Table I). The transition strength of the $(3^+) \rightarrow 2^+$ transition was measured to be $B(E2)\uparrow = 230(41)$ e^2fm^4 and $B(E2)\uparrow = 320(100)$ e^2fm^4 in the present experiment, using the ^{104}Pd and ^{120}Sn target, respectively. These values exceed both the previously measured $B(E2)\uparrow = 147(21)$ e^2fm^4 value published by Ettenauer *et al.* [31] and the MCSM predictions, which yield 168 e^2fm^4 [26]. The possible (4^+) state at 925 keV has a strong coupling to the deformed ground state with $B(E2, 2^+ \rightarrow (4^+)) = 125(45)$ e^2fm^4 [$B(E2)\uparrow = 96(50)$ e^2fm^4 for the ^{120}Sn target], in agreement with MCSM calculations, which yielded $B(E2)\uparrow = 90$ e^2fm^4. Compared to the rotational band structure of the $N = 19$ isotone ^{31}Mg [23] the $K = 2$ band of ^{30}Na seems to be less connected by $M1$ transitions. The $B(M1, (4^+) \rightarrow (3^+))$ value yielded 0.027(14) μ_N^2 and 0.43 μ_N^2 for the present experiment and MCSM calculations [26], respectively. Despite these differences in the observed transition probabilities, the results of the new Coulomb-excitation experiment confirm the large quadrupole collectivity and, thus, the intruder dominated 2p2h configuration of the ground state, for the $N = 19$ Na isotope.

V. SUMMARY

To summarize, we have investigated the Coulomb excitation of the unstable, neutron-rich nuclei ^{29,30}Na. For ^{29}Na the results of previous experiments could be largely confirmed and extended. Deduced collective properties of the first excited states are well described by MCSM calculations using the SDPF-M interaction. The measured $B(E2)$ values support the idea that in the Na isotopic chain the ground-state wave function contains a significant intruder admixture already at $N = 18$, with $N = 19$ having an almost pure 2p2h deformed ground-state configuration. However, higher-lying

states that are, as predicted by theory, dominated by intruder configurations are hardly populated in the present Coulomb-excitation experiments. The ground-state transitions of the assigned $(3/2^+_2)$ state at 1588 keV in ^{29}Na is found to have a moderately large $B(E2)$ value. In ^{30}Na a candidate for the (4^+) state is identified at 925 keV by coincidence relations. Excitation strengths and energies are well described by the MCSM calculations. Deviations found for the branching ratios and $B(M1)$ values indicate the importance to investigate the properties of excited states of exotic nuclei in the vicinity of the island of inversion further and to improve the shell-model description of odd-odd nuclei.

ACKNOWLEDGMENTS

This work has been supported by the German BMBF under Contracts No. 06K-167, No. 06KY205I, No. 06DA9036I, No. 06MT9156, No. 05P09PKCI5, No. 05P12PKFNE, No. 05P12RDCIA, and No. 05P12RDCIB, by the FWO-Vlaanderen (Belgium), by the IAP Belgian Science Policy (BriX network (P7/12)), by the UK Science and Technology Funding Council, by the EUROpean Nuclear Structure Integrated Infrastructure Initiative (EURONS, RII3-CT-2004-506065), and by the European Nuclear Science and Applications Research (ENSAR) under Project No. 262010.

[1] C. Thibault *et al.*, Phys. Rev. C **12**, 644 (1975).
[2] X. Campi, H. Flocard, A. K. Kerman, and S. Koonin, Nucl. Phys. A **251**, 193 (1975).
[3] E. K. Warburton, J. A. Becker, and B. A. Brown, Phys. Rev. C **41**, 1147 (1990).
[4] T. Otsuka, R. Fujimoto, Y. Utsuno, B. A. Brown, M. Honma, and T. Mizusaki, Phys. Rev. Lett. **87**, 082502 (2001).
[5] T. Otsuka, Y. Utsuno, R. Fujimoto, B. A. Brown, M. Honma, and T. Mizusaki, Eur. Phys. J. A **13**, 69 (2002).
[6] T. Otsuka, Y. Utsuno, R. Fujimoto, B. A. Brown, M. Honma, and T. Mizusaki, Eur. Phys. J. A **15**, 151 (2002).
[7] T. Otsuka, T. Suzuki, R. Fujimoto, H. Grawe, and Y. Akaishi, Phys. Rev. Lett. **95**, 232502 (2005).
[8] T. Otsuka, M. Honma, and D. Abe, Nucl. Phys. A **788**, 3c (2007).
[9] Y. Utsuno, T. Otsuka, T. Mizusaki, and M. Honma, Phys. Rev. C **60**, 054315 (1999).
[10] K. Heyde and J. L. Wood, J. Phys. G **17**, 135 (1991).
[11] M. Yamagami and N. Van Giai, Phys. Rev. C **69**, 034301 (2004).
[12] R. Rodríguez-Guzmán, J. L. Egido, and L. M. Robledo, Nucl. Phys. A **709**, 201 (2002).
[13] S. Péru, M. Girod, and J. F. Berger, Eur. Phys. J. A **9**, 35 (2000).
[14] J. Terasaki, H. Flocard, P.-H. Heenen, and P. Bonche, Nucl. Phys. A **621**, 706 (1997).
[15] P.-G. Reinhard, D. J. Dean, W. Nazarewicz, J. Dobaczewski, J. A. Maruhn, and M. R. Strayer, Phys. Rev. C **60**, 014316 (1999).
[16] T. Motobayashi *et al.*, Phys. Lett. B **346**, 9 (1995).
[17] B. V. Pritychenko *et al.*, Phys. Rev. C **65**, 061304(R) (2002).
[18] K. Wimmer *et al.*, Phys. Rev. Lett. **105**, 252501 (2010).
[19] J. A. Church *et al.*, Phys. Rev. C **72**, 054320 (2005).
[20] H. Iwasaki *et al.*, Phys. Lett. B **522**, 227 (2001).
[21] G. Neyens *et al.*, Phys. Rev. Lett. **94**, 022501 (2005).
[22] F. Maréchal *et al.*, Phys. Rev. C **72**, 044314 (2005).
[23] M. Seidlitz *et al.*, Phys. Lett. B **700**, 181 (2011).
[24] M. Keim, AIP Conf. Proc. No. **455**, 50 (1998).
[25] M. Keim *et al.*, Eur. Phys. J. A **8**, 31 (2000).
[26] Y. Utsuno, T. Otsuka, T. Glasmacher, T. Mizusaki, and M. Honma, Phys. Rev. C **70**, 044307 (2004).
[27] V. Tripathi *et al.*, Phys. Rev. C **73**, 054303 (2006).
[28] V. Tripathi *et al.*, Phys. Rev. C **76**, 021301(R) (2007).
[29] A. M. Hurst *et al.*, Phys. Lett. B **674**, 168 (2009).
[30] B. V. Pritychenko *et al.*, Phys. Rev. C **66**, 024325 (2002).
[31] S. Ettenauer *et al.*, Phys. Rev. C **78**, 017302 (2008).
[32] D. Cline, Ann. Rev. Nucl. Part. Sci. **36**, 683 (1986).
[33] http://isolde.web.cern.ch/ISOLDE/
[34] D. Habs *et al.*, Hyperfine Interact. **129**, 43 (2000).
[35] M. Shamsuzzoha Basunia, Nucl. Data Sheets **113**, 909 (2012).
[36] M. Shamsuzzoha Basunia, Nucl. Data Sheets **111**, 2331 (2010).
[37] F. Wenander, Nucl. Phys. A **701**, 528 (2002).
[38] N. Warr *et al.*, Eur. Phys. J. A **49**, 40 (2013).
[39] A. N. Ostrowski *et al.*, Nucl. Instrum. Methods A **480**, 448 (2002).
[40] J. Eberth *et al.*, Prog. Part. Nucl. Phys. **46**, 389 (2001).
[41] A. H. M. Evensen *et al.*, Nucl. Instrum. Methods B **126**, 160 (1997).
[42] J. Blachot, Nucl. Data Sheets **108**, 2035 (2007).
[43] V. Tripathi *et al.*, Phys. Rev. Lett. **94**, 162501 (2005).
[44] T. Czosnyka, D. Cline, and C. Y. Wu, Bull. Am. Phys. Soc. **28**, 745 (1983).
[45] T. Czosnyka, D. Cline, and C. Y. Wu (unpublished).
[46] W. D. Hamilton, *The Electromagnetic Interaction in Nuclear Spectroscopy* (North-Holland, Amsterdam, 1975).
[47] Z. Elekes *et al.*, Phys. Rev. C **73**, 044314 (2006).